

# Predict and Reconstruct: Joint Objectives for Self-Supervised Language Representation Learning

Aimen Boukhari

École Nationale Supérieure d’Informatique (ESI), Algiers , Algeria  
[mn\\_boukhari@esi.dz](mailto:mn_boukhari@esi.dz)

## Abstract

Masked language modelling (MLM) has been the dominant pre-training objective for text encoders since BERT, yet it encourages representations that are strongly anchored to surface-form token identity rather than deeper semantic structure. Inspired by the success of Joint Embedding Predictive Architectures (JEPA) [LeCun, 2022] in vision and audio, we propose a hybrid pre-training objective that combines a JEPA-style latent-space prediction loss with an MLM reconstruction loss over a single shared encoder. A learnable scalar  $\lambda$  continuously balances the two objectives during training. We pre-train both a hybrid model and a pure-MLM baseline on English Wikipedia using identical architectures and compute budgets (NVIDIA H100). Extensive representation analysis across five GLUE benchmarks (SST-2, MRPC, MNLI, CoLA, STS-B) using four pooling strategies reveals that the hybrid encoder produces significantly more uniform embeddings (uniformity  $\leq -0.16$  vs.  $-0.05$  for MLM), exhibits richer spectral geometry under max pooling, encodes less surface-level lexical information, and achieves a better semantic-to-lexical balance. Despite similar linear-probe downstream accuracy, the geometric differences are consistent and significant, suggesting that the JEPA predictive objective reshapes the latent space in ways that standard accuracy metrics alone cannot capture. Code and checkpoints: <https://github.com/aymen-000/predict-reconstruct-language-models>

## 1 Introduction

Self-supervised learning (SSL) has transformed representation learning across modalities. In computer vision, contrastive methods such as SimCLR [Chen et al., 2020] and MoCo [He et al., 2020], followed by non-contrastive approaches like BYOL [Grill et al., 2020] and VICReg [Bardes et al., 2022], demonstrated that powerful visual features can be learned without labels. In speech and audio, wav2vec [Baevski et al., 2020] and data2vec [Baevski et al., 2022] showed that masked prediction in latent space generalises across modalities. These successes share a common principle: rather than reconstructing pixels or waveforms, the model learns to *predict abstract representations* of masked or future content.

Yann LeCun formalised this intuition in [LeCun, 2022], arguing that reconstruction-based objectives are fundamentally limited because they force the model to allocate capacity to irrelevant low-level details. The Joint Embedding Predictive Architecture (JEPA) avoids this by having a predictor network match the *target encoder’s latent representation* of the masked region, never reconstructing tokens in pixel or token space. The image instantiation I-JEPA [Assran et al., 2023] demonstrated on ImageNet that JEPA pre-training produces representations that generalise better with fewer labelled examples than masked autoencoders, and that learned features are more semantically structured as evidenced by linear probing.

In natural language processing, BERT [Devlin et al., 2019] established MLM as the standard SSL objective. While highly effective, MLM operates in token space: the model must predict the exact identity of masked tokens, incentivising the encoder to retain fine-grained lexical information at the expense of broader semantic structure. Several analyses have confirmed that BERT representations are highly contextualised yet remain sensitive to surface-form variation [Ethayarajh, 2019, Rogers et al., 2020]. SimCSE [Gao et al., 2021] and DeCLUTR [Giorgi et al., 2021] improved the *uniformity* of BERT-derived sentence embeddings through contrastive fine-tuning, confirming that the MLM objective alone does not fully exploit the embedding hypersphere.

A natural question therefore arises: can a JEPA-style latent prediction objective be combined with MLM to produce text encoders that encode semantics more robustly? A recent independent line of work, LLM-JEPA [Huang et al., 2025], explores applying JEPA principles to autoregressive language models. Our work is complementary: we study the *representation geometry* of small-to-medium encoders trained under hybrid versus pure-MLM objectives, providing the first systematic analysis using alignment/uniformity metrics, eigenspectrum analysis, effective rank, and probing classifiers across multiple GLUE tasks.

### Contributions.

1. We propose a hybrid pre-training architecture that jointly optimises a JEPA cosine prediction loss and an MLM cross-entropy loss through a single shared encoder with a learnable balance weight  $\lambda$ .

2. We conduct the first systematic geometric analysis of hybrid vs. MLM-only text encoders across five GLUE datasets and four pooling strategies using six complementary representation metrics.
3. We show that hybrid training consistently improves embedding uniformity and spectral richness while reducing surface-form bias, even under a small pre-training budget.
4. We release code and model checkpoints to facilitate reproduction and extension of this analysis.

## 2 Background and Related Work

### 2.1 Reconstruction-Based SSL and Its Limitations

Masked language modelling, introduced in BERT [Devlin et al., 2019], predicts masked tokens from context. This objective is effective but carries an implicit bias: the model must memorise token-level statistics to recover the correct token identity, encouraging representations to retain lexical surface form rather than semantic content. LeCun [2022] identifies reconstruction objectives as fundamentally misaligned with the goal of learning abstract world models: predicting every detail of the input wastes model capacity on unpredictable or irrelevant information. In vision, masked autoencoders (MAE) [He et al., 2022] achieve strong results but require fine-tuning to match JEPA-style methods on linear evaluation [Assran et al., 2023], consistent with the hypothesis that pixel reconstruction does not optimally produce semantic features.

### 2.2 JEPA and Latent Prediction

I-JEPA [Assran et al., 2023] instantiates LeCun’s JEPA framework for images: a context encoder processes visible patches, a predictor maps context representations to target representations, and the target encoder (updated via exponential moving average, EMA) produces representations of masked regions that the predictor must match. The loss is computed in representation space rather than pixel space, avoiding the reconstruction trap. V-JEPA [Bardes et al., 2024] extends this to video and MC-JEPA [Bardes et al., 2023] adds motion consistency. LLM-JEPA [Huang et al., 2025] recently proposed adapting JEPA to autoregressive language models. Our work differs in focus: we study encoder representation geometry rather than downstream generation quality, and provide direct comparison with a controlled MLM baseline.

### 2.3 Representation Quality Metrics

Wang and Isola [2020] introduced *alignment* and *uniformity* for evaluating sentence embeddings on the  $\ell_2$ -normalised hypersphere. Roy and Vetterli [2007] defined the *effective rank* as the exponential of the Shannon entropy of the normalised

Hybrid Predict-and-Reconstruct Architecture

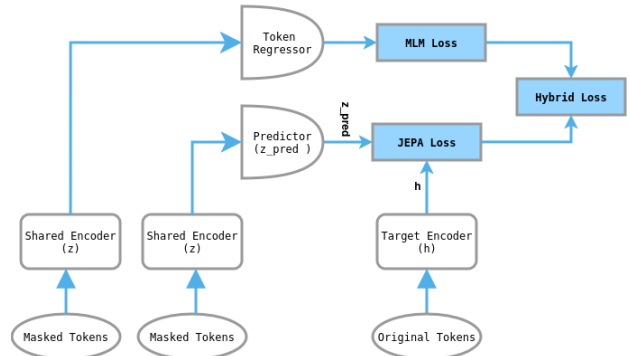


**Figure 1:** Hybrid Predict-and-Reconstruct architecture. The shared encoder produces contextual representations used by two branches: a predictor for the JEPA objective and a token regression head for the MLM objective. The target encoder is updated using exponential moving average (EMA) and provides stable targets for representation prediction.

singular-value distribution. Vershynin [2018] introduces the *stable rank* as a robust alternative. Garrido et al. [2023] used eigenspectrum analysis to compare contrastive and non-contrastive SSL objectives. Conneau and Kiela [2018] established the probing task framework for analysing what linguistic information is encoded in sentence representations, and Ethayarajh [2019] applied contextuality analysis to BERT representations.

## 3 Method

### 3.1 Architecture Overview

Our architecture consists of three components: a shared encoder  $f_\theta$ , a predictor  $g_\phi$ , and a target encoder  $\tilde{f}_\theta$  updated via EMA. The shared encoder processes input tokens and produces contextualised representations used for both the JEPA and MLM objectives. A lightweight token regressor  $h_\psi$  maps encoder outputs to vocabulary logits for the MLM branch. The overall architecture is illustrated in Figure 1.

### 3.2 Hybrid Pre-training Objective

Given a token sequence  $\mathbf{x}$  of length  $L$ , we apply two distinct masking operations.

**Block masking (JEPA branch).** Following I-JEPA [Assran et al., 2023], we sample contiguous block masks. An encoder mask  $\mathcal{M}_{\text{enc}}$  (scale  $[0.65, 0.85]$ ) defines the visible context; prediction masks  $\{\mathcal{M}_{\text{pred}}^k\}_{k=1}^2$  (scale  $[0.10, 0.25]$ ) define the target regions.

**BERT masking (MLM branch).** We apply standard BERT-style masking with probability  $p = 0.15$ : 80% of selected positions receive the [MASK] token, 10% are replaced by a random token, and 10% are left unchanged.

**Forward pass.**

$$\mathbf{z} = f_{\theta}(\tilde{\mathbf{x}}, \mathcal{M}_{\text{enc}}) \quad (1)$$

$$\hat{\mathbf{h}} = g_{\phi}(\mathbf{z}, \mathcal{M}_{\text{enc}}, \mathcal{M}_{\text{pred}}) \quad (2)$$

$$\mathbf{h} = f_{\theta}(\mathbf{x}) \quad (\text{no grad}) \quad (3)$$

$$\mathbf{z}_{\text{full}} = f_{\theta}(\tilde{\mathbf{x}}) \quad (4)$$

where  $\tilde{\mathbf{x}}$  denotes the BERT-masked token sequence,  $\mathbf{h}$  is the target representation, and  $\mathbf{z}_{\text{full}}$  is the full-sequence latent used for token regression.

**Loss functions.**

$$\mathcal{L}_{\text{JEPA}} = 1 - \frac{1}{|\mathcal{B}|} \sum_{(i,j) \in \mathcal{B}} \cos(\hat{\mathbf{h}}_{ij}, \mathbf{h}_{ij}) \quad (5)$$

$$\mathcal{L}_{\text{MLM}} = \text{CE}(h_{\psi}(\mathbf{z}_{\text{full}}), \mathbf{y}_{\text{mask}}) \quad (6)$$

$$\mathcal{L} = \lambda \mathcal{L}_{\text{JEPA}} + (1 - \lambda) \mathcal{L}_{\text{MLM}}, \quad \lambda = \sigma(w) \quad (7)$$

where  $w \in \mathbb{R}$  is a learnable scalar optimised end-to-end and  $\sigma$  is the sigmoid function.

**EMA update.**

$$\bar{\theta} \leftarrow m \bar{\theta} + (1 - m) \theta, \quad m \in [0.996, 1.0] \quad (8)$$

### 3.3 Token Regressor

The token regressor  $h_{\psi}$  operates directly on the shared encoder’s latent representation:

$$h_{\psi}(\mathbf{z}) = W_2 \text{LN}(\text{GELU}(W_1 \mathbf{z})) \quad (9)$$

with  $W_1 \in \mathbb{R}^{D \times D}$ ,  $W_2 \in \mathbb{R}^{D \times V}$  ( $V = \text{vocabulary size}$ ) and  $\text{LN}(\cdot)$  denotes layer normalisation [Ba et al., 2016]. Unlike a standard MLM head,  $h_{\psi}$  receives gradients from both objectives through the shared encoder weights.

### 3.4 Sentence Pooling

For downstream evaluation, token representations are aggregated via mean pooling over non-padding positions:

$$\mathbf{s} = \frac{\sum_{t=1}^L \mathbf{1}[x_t \neq \text{pad}] \mathbf{z}_t}{\sum_{t=1}^L \mathbf{1}[x_t \neq \text{pad}]} \quad (10)$$

This matches the pooling used in all linear-probe fine-tuning experiments.

## 4 Experimental Setup

### 4.1 Pre-training

**Data.** Both models are pre-trained on English Wikipedia (WikiText). All text is tokenised with the `bert-base-uncased` tokeniser (vocabulary size 30,522) and sequences are truncated or padded to 512 tokens.

**Model architecture.** The model uses a transformer-based encoder with token embedding dimension  $d_{\text{emb}} = 512$ . The predictor consists of 6 layers with embedding dimension  $d_{\text{pred}} = 512$ . A target encoder, with the same architecture as the main encoder, is maintained with frozen weights and updated via exponential moving average. The token regressor head maps the encoder outputs back to the vocabulary (`vocab.size = 30,522`) for masked language modeling. Optimization is performed with AdamW, using a learnable scalar to balance the JEPA (cosine) and MLM (cross-entropy) losses.

**Training.** Both models are trained for 3 epochs with batch size 64 on a single NVIDIA H100 GPU using bfloat16 mixed precision and AdamW with cosine learning rate schedule (peak LR  $5 \times 10^{-5}$ , weight decay 0.05). Full hyperparameters are given in Table 1.

**Table 1:** Pre-training hyperparameters.

Hyperparameter	Value
Epochs	3
Batch size	64
Peak LR	$5 \times 10^{-5}$
LR schedule	cosine
Warmup steps	10
Weight decay	0.05
Precision	bfloat16
EMA range	[0.996, 1.0]
Encoder mask scale	[0.65, 0.85]
Pred. mask scale	[0.10, 0.25]
Num. pred. masks	2
Min. keep tokens	32
MLM probability	0.15
Hardware	NVIDIA H100

### 4.2 Downstream Evaluation: Linear Probing

We evaluate frozen encoder representations via linear probing on five GLUE tasks [Wang et al., 2018]. The encoder is kept frozen throughout; only a lightweight head is trained. Since GLUE test labels are not publicly available, all results are reported on the official validation splits. No hyperparameter search was performed on the validation set; the same configuration was applied to both models.

**Single-sentence tasks (SST-2, CoLA).** Mean-pooled representations feed a LayerNorm  $\rightarrow$  Dropout(0.2)  $\rightarrow$  Linear head.

**Sentence-pair tasks (MRPC, MNLI).** Both sentences are encoded independently; the classifier receives  $[\mathbf{s}_1; \mathbf{s}_2; |\mathbf{s}_1 - \mathbf{s}_2|; \mathbf{s}_1 \odot \mathbf{s}_2]$  [Conneau et al., 2017].

**Regression task (STS-B).** Cosine similarity is calibrated to the  $[0, 5]$  score range via a learnable scale and bias:  $\hat{y} = \sigma_w \cdot \cos(\mathbf{s}_1, \mathbf{s}_2) + b_w$ .

Per-task fine-tuning details are given in Table 2.

**Table 2:** Fine-tuning hyperparameters per task.

Task	LR	Epochs	Metric
SST-2	$1 \times 10^{-3}$	90	Accuracy
MRPC	$1 \times 10^{-3}$	10	F1
MNLI	$1 \times 10^{-3}$	15	Acc. (matched)
STS-B	$1 \times 10^{-3}$	15	Spearman $\rho$

### 4.3 Representation Analysis

We extract frozen sentence embeddings for up to 2,000 samples from each task’s validation split and compute six metrics:

- Spectral entropy** [Garrido et al., 2023]:  $H_{\text{spec}} = H(\boldsymbol{\sigma} / \|\boldsymbol{\sigma}\|_1) / \log D$ .
- Effective rank** [Roy and Vetterli, 2007]:  $\text{erank} = \exp H(\boldsymbol{\sigma} / \|\boldsymbol{\sigma}\|_1)$ .
- Stable rank** [Vershynin, 2018]:  $\text{srnk} = \|\mathbf{Z}\|_F^2 / \|\mathbf{Z}\|_2^2$ .
- Alignment** [Wang and Isola, 2020]: mean squared  $\ell_2$  distance between same-class pairs.
- Uniformity** [Wang and Isola, 2020]:  $\log \mathbb{E}[e^{-2\|\mathbf{u}-\mathbf{v}\|^2}]$  on  $\ell_2$ -normalised embeddings.
- Probe gap** [Conneau and Kiela, 2018]: semantic probe accuracy minus token probe accuracy.

All metrics are computed under four pooling strategies: mean, max, weighted mean, and attention pooling. Full formal definitions are given in Appendix D.

## 5 Results

### 5.1 Downstream Task Accuracy

Table 3 reports linear-probe performance on five GLUE tasks. Both models achieve comparable accuracy, consistent with the known finding that MLM baselines are strong linear classifiers under mean-pooled representations [Gao et al., 2021].

**Table 3:** Linear-probe downstream performance on GLUE validation splits. Frozen encoder; best per-task result in **bold**. Spearman  $\rho$  for STS-B.

Task	Hybrid	MLM-only
SST-2 (Acc.)	67.55	<b>68.69</b>
MRPC (F1)	<b>63.09</b>	59.84
MNLI (Acc.)	50.82	<b>51.36</b>
STS-B <sup>†</sup> (Spearman)	0.281	<b>0.283</b>

## 5.2 Representation Geometry

### 5.2.1 Uniformity

The hybrid encoder consistently achieves significantly more negative uniformity scores across all five datasets and all four pooling strategies (Table 4). The mean uniformity under attention pooling is  $-0.54$  for hybrid vs.  $-0.07$  for MLM-only — a sevenfold difference. This confirms that the JEPa predictive objective prevents representational collapse and promotes a more isotropic use of the embedding hypersphere [Wang and Isola, 2020], analogous to findings in vision [Assran et al., 2023].

**Table 4:** Uniformity ( $\downarrow$  better) by dataset and pooling.

Dataset	Pooling	Hybrid	MLM
SST-2	mean	<b>-0.160</b>	-0.052
	max	<b>-0.294</b>	-0.090
	weighted	<b>-0.160</b>	-0.052
	attention	<b>-0.448</b>	-0.055
MRPC	mean	<b>-0.134</b>	-0.053
	max	<b>-0.262</b>	-0.088
	weighted	<b>-0.134</b>	-0.053
	attention	<b>-0.269</b>	-0.055
MNLI	mean	<b>-0.169</b>	-0.063
	max	<b>-0.290</b>	-0.096
	weighted	<b>-0.163</b>	-0.063
	attention	<b>-0.365</b>	-0.067
CoLA	mean	<b>-0.314</b>	-0.079
	max	<b>-0.365</b>	-0.098
	weighted	<b>-0.314</b>	-0.079
	attention	<b>-0.955</b>	-0.083
STS-B	mean	<b>-0.202</b>	-0.067
	max	<b>-0.321</b>	-0.102
	weighted	<b>-0.201</b>	-0.068
	attention	<b>-0.577</b>	-0.069

### 5.2.2 Alignment–Uniformity Trade-off

The improved uniformity comes at the cost of higher within-class alignment values for hybrid representations. MLM-only alignment is consistently near zero ( $\leq 0.002$ ), indicating extremely tight class clusters, while hybrid alignment is larger

(e.g. SST-2/attention: 0.20 vs. 0.001), reflecting a more relaxed intra-class structure. This alignment-uniformity trade-off [Wang and Isola, 2020] directly explains why linear-probe accuracy is similar for both models: linear classifiers benefit primarily from tight clusters, which favours MLM-only representations. Scatter plots of alignment vs. uniformity and intra/inter-class distance ratios for all datasets are given in Appendix B.

### 5.2.3 Spectral Analysis

Under max pooling, the hybrid encoder achieves higher spectral entropy and effective rank across all datasets (Table 5), indicating that more embedding dimensions carry meaningful variance. The stable rank is also consistently higher for hybrid under max pooling.

**Table 5:** Spectral metrics under max pooling. H=Hybrid; M=MLM-only. Eff. Rank [Roy and Vetterli, 2007]; Srank [Vershynin, 2018].

Task	Spec. Ent. ( $\uparrow$ )		Eff. Rank ( $\uparrow$ )		Srank ( $\uparrow$ )	
	H	M	H	M	H	M
SST-2	<b>0.765</b>	0.735	<b>384</b>	364	<b>6.98</b>	4.11
MRPC	0.794	<b>0.824</b>	299	<b>301</b>	8.18	<b>11.33</b>
MNLI	<b>0.779</b>	0.767	<b>406</b>	391	<b>8.35</b>	4.99
CoLA	<b>0.752</b>	0.715	<b>365</b>	330	<b>10.82</b>	4.75
STS-B	<b>0.743</b>	0.721	<b>390</b>	372	<b>6.94</b>	4.09

### 5.2.4 Probing Results

**Token probe.** The hybrid encoder consistently exhibits lower token probe accuracy (Table 6), indicating that its representations retain less surface-level lexical information. Across all tasks under attention pooling, hybrid token accuracy is 3–9 points lower than MLM-only.

**Semantic probe.** Despite encoding less token-level information, hybrid representations achieve comparable or slightly higher semantic probe performance. Under max pooling on MRPC, hybrid achieves the only positive probe gap (+0.031), confirming that the JEPA objective promotes semantic encoding over lexical memorisation.

**CoLA MCC.** The hybrid encoder achieves consistently positive MCC on CoLA (0.052–0.064 vs.  $-0.023$ – $-0.010$  for MLM), suggesting that block-span prediction induces a weak but reproducible syntactic sensitivity absent from token-level MLM.

## 6 Ablation Study: Pooling Strategies

We evaluate four pooling strategies to disentangle the effect of aggregation from the effect of the pre-training objective.

**Table 6:** Probing results under attention pooling. H=Hybrid; M=MLM-only.

Task	Token ( $\downarrow$ )		Semantic ( $\uparrow$ )		Gap ( $\uparrow$ )	
	H	M	H	M	H	M
SST-2	<b>0.663</b>	0.754	<b>0.643</b>	0.635	<b>-0.019</b>	-0.119
MRPC	<b>0.616</b>	0.678	0.608	<b>0.610</b>	<b>-0.008</b>	-0.068
MNLI	<b>0.685</b>	0.740	0.326	<b>0.333</b>	<b>-0.359</b>	-0.407
CoLA	<b>0.813</b>	0.870	<b>0.602</b>	0.594	<b>-0.211</b>	-0.276
STS-B	<b>0.592</b>	0.654	0.187	<b>0.193</b>	<b>-0.405</b>	-0.460

**Mean pooling** (Eq. 10) is the default and matches the pooling used during fine-tuning. It provides the fairest comparison for downstream accuracy but yields the most compressed spectral geometry.

**Max pooling** consistently yields the highest spectral entropy and effective rank for both models. It is the most discriminative strategy for the hybrid encoder on classification tasks, and the only configuration under which the probe gap turns positive for MRPC.

**Weighted mean pooling** produces results nearly identical to mean pooling across all metrics. Since weights are initialised uniformly and evaluated inside `no_grad`, this serves as a useful null result confirming that observed geometric differences are intrinsic to the encoder rather than to the pooling arithmetic.

**Attention pooling** amplifies differences between the two models more than any other strategy. The uniformity gap is widest under attention pooling (SST-2:  $-0.448$  vs.  $-0.055$ ; STS-B:  $-0.577$  vs.  $-0.069$ ), suggesting that the JEPA objective most strongly affects high-attention positions — the tokens the model considers most semantically salient.

Figure 2 illustrates the pooling ablation for the hybrid encoder on SST-2.

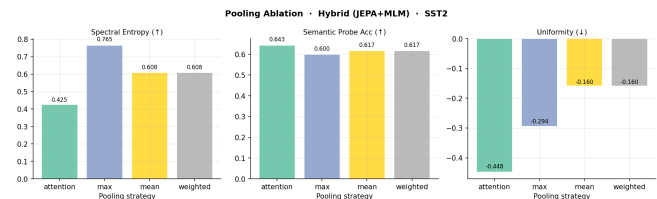


**Figure 2:** Spectral entropy, semantic probe accuracy, and uniformity for the hybrid encoder under four pooling strategies on SST-2. Max pooling maximises spectral richness; attention pooling maximises the uniformity advantage.

## 7 Discussion

**Why similar accuracy despite different geometry?** The alignment-uniformity trade-off [Wang and Isola, 2020] provides the explanation. Hybrid representations cover the embedding hypersphere more uniformly but do not cluster same-class points as tightly. Since linear classifiers benefit primarily from tight clusters, MLM’s alignment advantage offsets hybrid’s uniformity advantage at the linear-probe evaluation level. We expect the uniformity advantage to translate to downstream gains under non-linear probing, retrieval tasks, or longer pre-training.

**Attention pooling as a diagnostic tool.** The amplified differences under attention pooling suggest that JEPA’s effect is concentrated at salient positions rather than distributed uniformly across the sequence, consistent with the block-masking design that forces the predictor to recover representations of contiguous spans.

**Resource constraints.** Pre-training was intentionally limited to 3 epochs on a modest corpus to study the effect of the objective under a controlled compute budget. The geometric differences observed are therefore likely a lower bound on what is achievable at scale.

## 8 Future Work

- **Alternative prediction losses.** Cosine similarity enforces directional alignment but ignores magnitude. Future work should evaluate smooth  $\ell_1$ , VICReg [Bardes et al., 2022], or Barlow Twins [Zbontar et al., 2021] losses in the JEPA branch.
- **Curriculum-based  $\lambda$ .** The current  $\lambda$  converges slowly. A schedule starting MLM-heavy and shifting to JEPA-heavy as the target encoder matures may accelerate learning.
- **Alternative masking strategies.** Span masking [Joshi et al., 2020], whole-word masking, and syntactically informed masking are natural alternatives.
- **Scale.** Extending to BookCorpus + Wikipedia, more epochs, and larger model sizes is the most direct path to assessing whether geometric advantages translate to accuracy improvements.
- **Non-linear probing and retrieval.** Evaluating with MLP probes and semantic similarity benchmarks (STS12–STS16, SICK-R) would provide a more complete picture.
- **Collapse monitoring.** Online tracking of uniformity and effective rank during training could serve as an adaptive objective-switching signal.

## 9 Conclusion

We proposed a hybrid pre-training objective that combines a JEPA-style latent prediction loss with masked language modelling over a single shared encoder. Through systematic representation analysis across five GLUE benchmarks and four pooling strategies, we showed that the hybrid objective consistently produces more uniform embedding distributions, richer spectral geometry, and better semantic-to-lexical balance compared to a controlled MLM-only baseline trained under identical conditions. These advantages are not captured by linear-probe accuracy alone, highlighting the value of geometric representation analysis as a complementary evaluation protocol. Our findings provide empirical support for LeCun’s hypothesis that latent-space prediction objectives lead to more abstract representations than token reconstruction [LeCun, 2022], and constitute a step toward understanding how JEPA principles can be applied to language encoders under realistic resource constraints.

## References

- M. Assran, Q. Duval, I. Misra, P. Bojanowski, P. Vincent, M. Rabbat, Y. LeCun, and N. Ballas. Self-supervised learning from images with a joint-embedding predictive architecture. In *CVPR 2023*, 2023.
- J.L. Ba, J.R. Kiros, and G.E. Hinton. Layer normalization. *arXiv:1607.06450*, 2016.
- A. Baeovski, H. Zhou, A. Mohamed, and M. Auli. wav2vec 2.0: A framework for self-supervised learning of speech representations. In *NeurIPS 2020*, 2020.
- A. Baeovski, W.-N. Hsu, Q. Xu, A. Babu, J. Gu, and M. Auli. data2vec: A general framework for self-supervised learning in speech, vision and language. In *ICML 2022*, 2022.
- A. Bardes, J. Ponce, and Y. LeCun. Vicreg: Variance-invariance-covariance regularization for self-supervised learning. In *ICLR 2022*, 2022.
- A. Bardes, J. Ponce, and Y. LeCun. Mc-jeпа: A joint-embedding predictive architecture for self-supervised learning of motion and content features. *arXiv preprint arXiv:2307.12698*, 2023.
- A. Bardes, Q. Garrido, J. Ponce, M. Rabbat, Y. LeCun, M. Assran, and N. Ballas. Revisiting feature prediction for learning visual representations from video. *arXiv:2404.08471*, 2024.
- T. Chen, S. Kornblith, M. Norouzi, and G. Hinton. A simple framework for contrastive learning of visual representations. In *ICML 2020*, 2020.
- A. Conneau and D. Kiela. Senteval: An evaluation toolkit for universal sentence representations. In *LREC 2018*, 2018.

- A. Conneau, D. Kiela, H. Schwenz, L. Barrault, and A. Bordes. Supervised learning of universal sentence representations from natural language inference data. In *EMNLP 2017*, 2017.
- J. Devlin, M.-W. Chang, K. Lee, and K. Toutanova. Bert: Pre-training of deep bidirectional transformers for language understanding. In *NAACL 2019*, 2019.
- K. Ethayarajh. How contextual are contextualized word representations? comparing the geometry of bert, elmo, and gpt-2 embeddings. In *EMNLP 2019*, 2019.
- T. Gao, X. Yao, and D. Chen. Simcse: Simple contrastive learning of sentence embeddings. In *EMNLP 2021*, 2021.
- Q. Garrido, Y. Chen, A. Bardes, L. Najman, and Y. LeCun. On the duality between contrastive and non-contrastive self-supervised learning. In *ICLR 2023*, 2023.
- J. Giorgi, O. Nitski, B. Wang, and G. Bader. Declutr: Deep contrastive learning for unsupervised textual representations. In *ACL 2021*, 2021.
- J.-B. Grill, F. Strub, F. Alché, et al. Bootstrap your own latent: A new approach to self-supervised learning. In *NeurIPS 2020*, 2020.
- K. He, H. Fan, Y. Wu, S. Xie, and R. Girshick. Momentum contrast for unsupervised visual representation learning. In *CVPR 2020*, 2020.
- K. He, X. Chen, S. Xie, Y. Li, P. Dollár, and R. Girshick. Masked autoencoders are scalable vision learners. In *CVPR 2022*, 2022.
- H. Huang, Y. LeCun, and R. Balestriero. Llm-jepa: Large language models meet joint embedding predictive architectures. *arXiv preprint arXiv:2509.14252*, 2025.
- M. Joshi, D. Chen, Y. Liu, D.S. Weld, L. Zettlemoyer, and O. Levy. Spanbert: Improving pre-training by representing and predicting spans. 2020.
- Y. LeCun. A path towards autonomous machine intelligence. OpenReview preprint, 2022.
- A. Rogers, O. Kovaleva, and A. Rumshisky. A primer in bertology: What we know about how bert works. *TACL 2020*, 2020.
- O. Roy and M. Vetterli. The effective rank: A measure of effective dimensionality. In *EUSIPCO 2007*, 2007.
- R. Vershynin. *High-Dimensional Probability*. Cambridge University Press, 2018.
- A. Wang, A. Singh, J. Michael, F. Hill, O. Levy, and S. Bowman. Glue: A multi-task benchmark and analysis platform for natural language understanding. In *ICLR 2019*, 2018.
- T. Wang and P. Isola. Understanding contrastive representation learning through alignment and uniformity on the hypersphere. In *ICML 2020*, 2020.
- J. Zbontar, L. Jing, I. Misra, Y. LeCun, and S. Deny. Barlow twins: Self-supervised learning via redundancy reduction. In *ICML 2021*, 2021.

## A Full Representation Analysis Tables

Tables 7–11 report all six representation metrics for all pooling strategies across all datasets. H = Hybrid; M = MLM-only.

**Table 7:** Full representation metrics — SST-2.

Pool	Spec. Ent.		Eff. Rank		Srank		Uniformity		Sem. Probe		Probe Gap	
	H	M	H	M	H	M	H	M	H	M	H	M
mean	<b>0.609</b>	0.605	242	249	4.49	4.50	<b>-0.160</b>	-0.052	0.617	0.618	<b>-0.138</b>	-0.152
max	<b>0.765</b>	0.735	<b>384</b>	364	<b>6.98</b>	4.11	<b>-0.294</b>	-0.090	<b>0.600</b>	0.595	<b>-0.008</b>	-0.045
weighted	<b>0.609</b>	0.605	242	249	4.49	4.50	<b>-0.160</b>	-0.052	0.617	0.619	<b>-0.139</b>	-0.149
attention	0.425	0.602	231	255	1.81	4.15	<b>-0.448</b>	-0.055	<b>0.643</b>	0.635	<b>-0.019</b>	-0.119

**Table 8:** Full representation metrics — MRPC.

Pool	Spec. Ent.		Eff. Rank		Srank		Uniformity		Sem. Probe		Probe Gap	
	H	M	H	M	H	M	H	M	H	M	H	M
mean	<b>0.631</b>	0.629	184	186	7.39	7.94	<b>-0.134</b>	-0.053	0.583	0.635	-0.052	-0.038
max	0.794	<b>0.824</b>	299	301	8.18	11.33	<b>-0.262</b>	-0.088	<b>0.618</b>	0.576	<b>+0.031</b>	-0.002
weighted	<b>0.631</b>	0.629	184	186	7.39	7.94	<b>-0.134</b>	-0.053	0.583	0.635	-0.057	-0.038
attention	0.611	<b>0.642</b>	<b>198</b>	194	4.13	8.73	<b>-0.269</b>	-0.055	0.608	<b>0.610</b>	<b>-0.008</b>	-0.068

**Table 9:** Full representation metrics — MNLI.

Pool	Spec. Ent.		Eff. Rank		Srank		Uniformity		Sem. Probe		Probe Gap	
	H	M	H	M	H	M	H	M	H	M	H	M
mean	<b>0.607</b>	0.597	242	245	<b>6.06</b>	5.83	<b>-0.169</b>	-0.063	<b>0.362</b>	0.354	<b>-0.392</b>	-0.410
max	<b>0.779</b>	0.767	<b>406</b>	391	<b>8.35</b>	4.99	<b>-0.290</b>	-0.096	0.315	<b>0.349</b>	-0.310	-0.288
weighted	<b>0.607</b>	0.597	242	245	<b>6.06</b>	5.83	<b>-0.163</b>	-0.063	<b>0.363</b>	0.355	<b>-0.392</b>	-0.409
attention	0.538	<b>0.603</b>	253	253	2.76	<b>5.91</b>	<b>-0.365</b>	-0.067	0.326	<b>0.333</b>	-0.359	-0.407

**Table 10:** Full representation metrics — CoLA. Semantic probe reports MCC.

Pool	Spec. Ent.		Eff. Rank		Srank		Uniformity		MCC ( $\uparrow$ )		Probe Gap	
	H	M	H	M	H	M	H	M	H	M	H	M
mean	<b>0.606</b>	0.586	235	239	<b>5.16</b>	4.58	<b>-0.314</b>	-0.079	<b>0.064</b>	0.000	<b>-0.246</b>	-0.284
max	<b>0.752</b>	0.715	<b>365</b>	330	<b>10.82</b>	4.75	<b>-0.365</b>	-0.098	<b>0.024</b>	-0.023	<b>-0.224</b>	-0.306
weighted	<b>0.606</b>	0.586	235	239	<b>5.16</b>	4.58	<b>-0.314</b>	-0.079	<b>0.064</b>	0.000	<b>-0.246</b>	-0.285
attention	0.479	<b>0.572</b>	221	<b>241</b>	2.20	<b>3.91</b>	<b>-0.955</b>	-0.083	<b>0.052</b>	0.010	<b>-0.211</b>	-0.276

**Table 11:** Full representation metrics — STS-B. Semantic probe reports Spearman  $\rho$ .

Pool	Spec. Ent.		Eff. Rank		Srank		Uniformity		Spearman ( $\uparrow$ )		Probe Gap	
	H	M	H	M	H	M	H	M	H	M	H	M
mean	0.581	<b>0.588</b>	228	235	4.83	5.53	<b>-0.202</b>	-0.067	<b>0.284</b>	0.224	<b>-0.369</b>	-0.449
max	<b>0.743</b>	0.721	<b>390</b>	372	<b>6.94</b>	4.09	<b>-0.321</b>	-0.102	0.140	<b>0.167</b>	<b>-0.376</b>	-0.397
weighted	0.581	<b>0.588</b>	227	235	4.83	5.53	<b>-0.201</b>	-0.068	<b>0.284</b>	0.224	<b>-0.369</b>	-0.446
attention	0.484	<b>0.597</b>	233	<b>243</b>	2.35	<b>5.70</b>	<b>-0.577</b>	-0.069	0.187	<b>0.193</b>	<b>-0.405</b>	-0.460

## B Alignment–Uniformity Plots

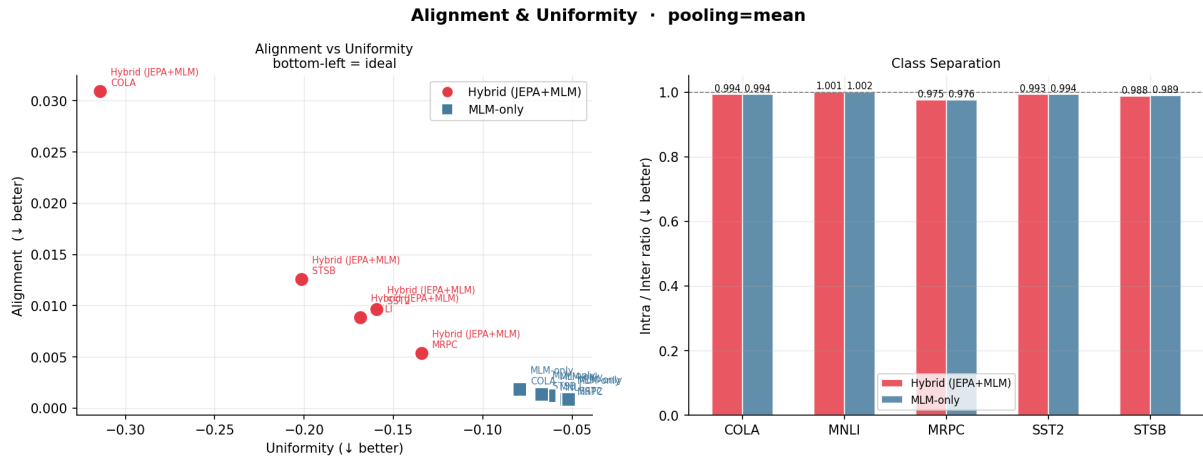


**Figure 3:** Alignment vs. uniformity and class separation — mean pooling, all datasets.

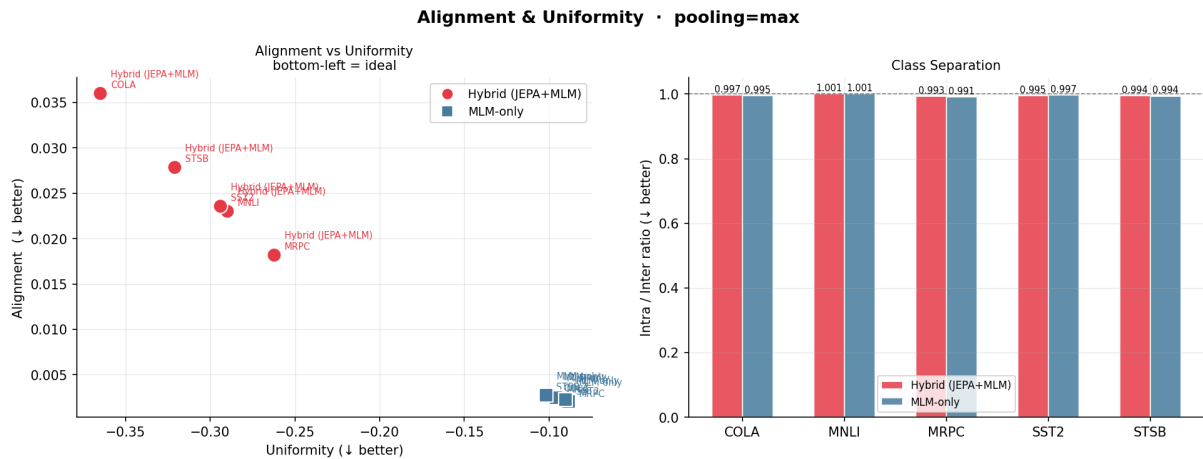


**Figure 4:** Alignment vs. uniformity and class separation — max pooling, all datasets.

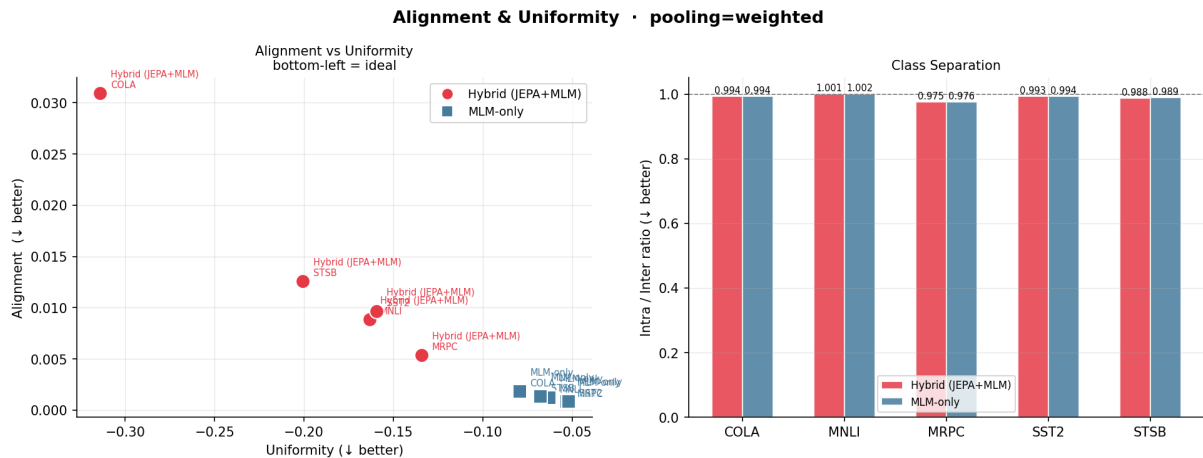


**Figure 5:** Alignment vs. uniformity and class separation — weighted mean pooling, all datasets.

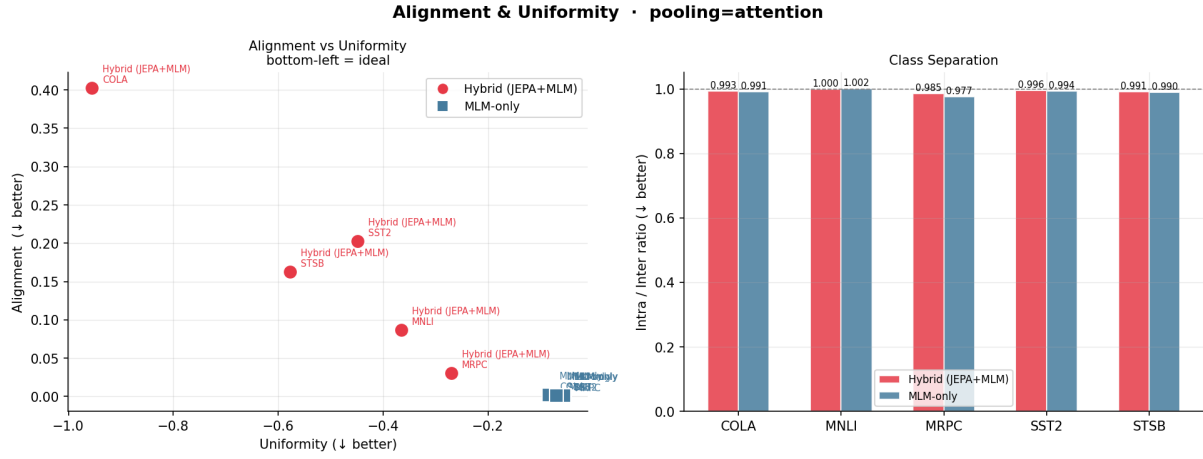


**Figure 6:** Alignment vs. uniformity and class separation — attention pooling, all datasets. The uniformity gap between hybrid and MLM-only is most pronounced here, consistent with the quantitative results in Table 4.

## C Eigenspectrum Plots

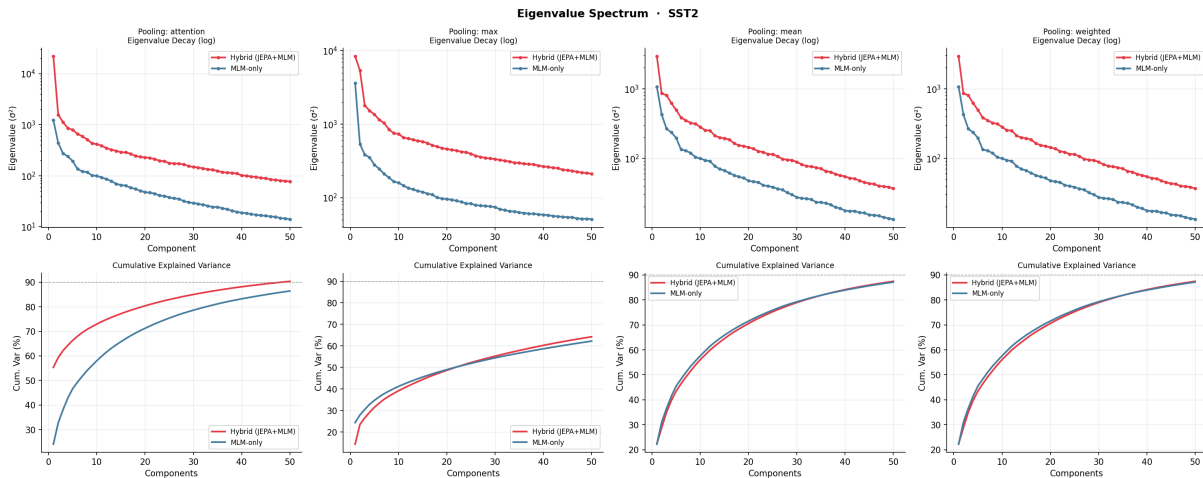


**Figure 7:** Eigenspectrum — SST-2, mean pooling.

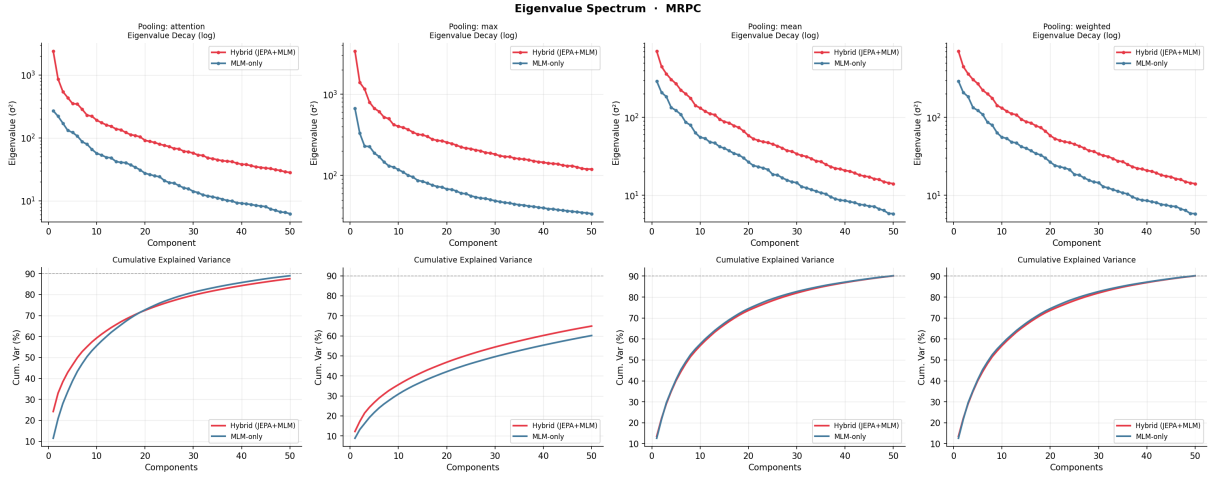


**Figure 8:** Eigenvalue spectrum — MRPC, mean pooling.

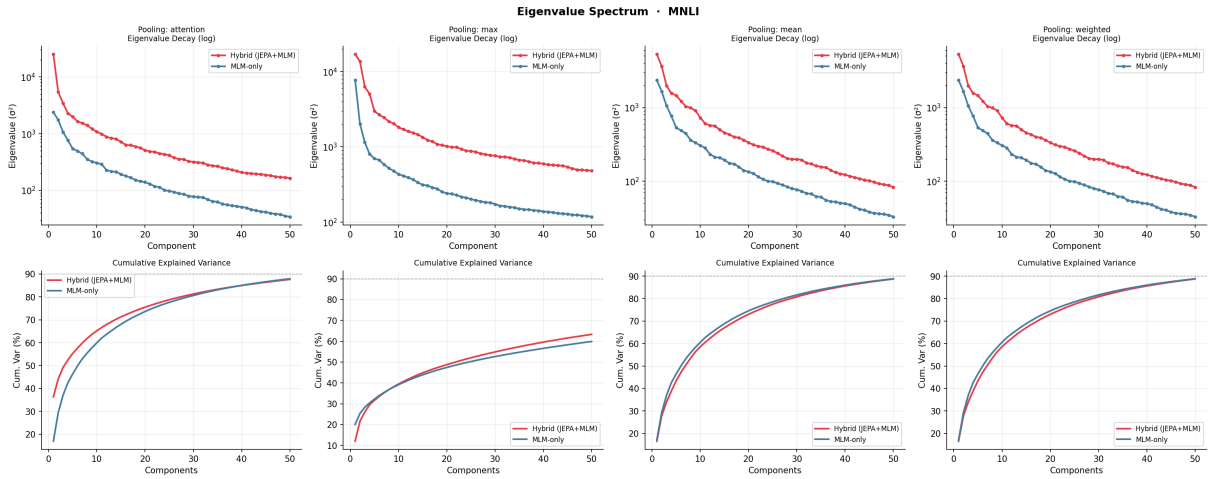


**Figure 9:** Eigenvalue spectrum — MNLi, mean pooling.

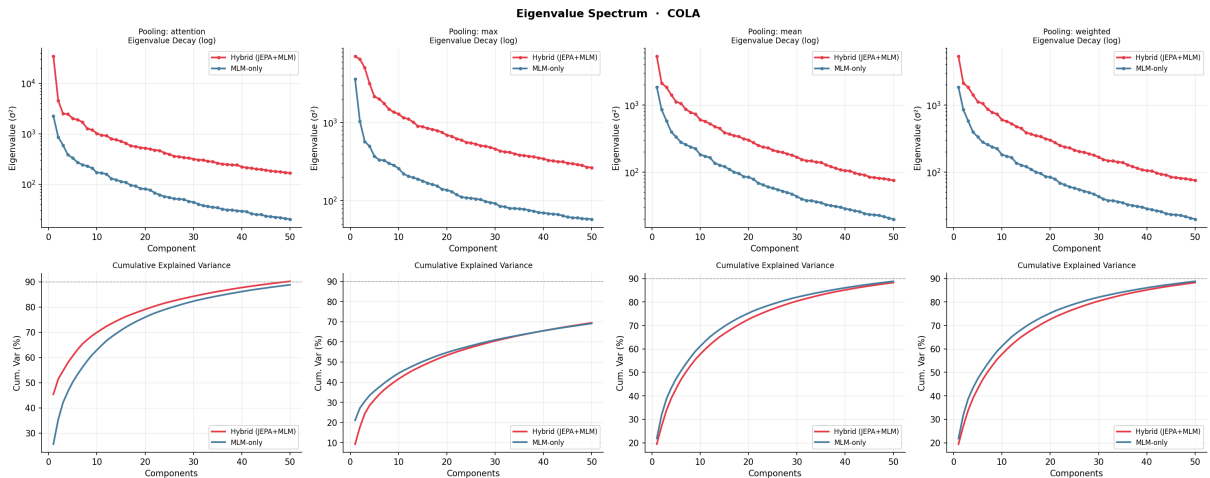


**Figure 10:** Eigenvalue spectrum — CoLA, mean pooling.

## D Representation Metric Definitions

Let  $\mathbf{Z} \in \mathbb{R}^{N \times D}$  denote the centred embedding matrix, and let  $\boldsymbol{\sigma} = (\sigma_1, \dots, \sigma_r)$  be its singular values in descending order. All metrics are computed on frozen sentence embeddings extracted from the validation split.

### 1. Spectral Entropy [Garrido et al., 2023].

$$H_{\text{spec}} = \frac{H(\boldsymbol{\sigma} / \|\boldsymbol{\sigma}\|_1)}{\log D}, \quad H(p) = -\sum_i p_i \log p_i \quad (11)$$

$H_{\text{spec}} \in [0, 1]$ ; a value of 1 means all singular values are equal, indicating that every embedding dimension carries the same variance (maximally rich representation).

### 2. Effective Rank [Roy and Vetterli, 2007].

$$\text{erank}(\mathbf{Z}) = \exp H(\boldsymbol{\sigma} / \|\boldsymbol{\sigma}\|_1) \quad (12)$$

Measures the number of dimensions that effectively contribute to the variance; higher values indicate richer representations.

### 3. Stable Rank [Vershynin, 2018].

$$\text{srank}(\mathbf{Z}) = \frac{\|\mathbf{Z}\|_F^2}{\|\mathbf{Z}\|_2^2} = \frac{\sum_i \sigma_i^2}{\sigma_1^2} \quad (13)$$

A robust alternative to effective rank that is less sensitive to outlier singular values.

### 4. Alignment [Wang and Isola, 2020].

$$\mathcal{A}(f; \alpha) = \mathbb{E}_{(\mathbf{u}, \mathbf{v}) \sim p_{\text{pos}}} [\|\hat{f}(\mathbf{u}) - \hat{f}(\mathbf{v})\|^2]^\alpha, \quad \alpha = 2 \quad (14)$$

where  $\hat{f}(\mathbf{x}) = f(\mathbf{x}) / \|f(\mathbf{x})\|_2$  and  $p_{\text{pos}}$  is the distribution of same-class pairs. Lower alignment means same-class representations cluster more tightly.

### 5. Uniformity [Wang and Isola, 2020].

$$\mathcal{U}(f; t) = \log \mathbb{E}_{\mathbf{u}, \mathbf{v} \stackrel{\text{i.i.d.}}{\sim} p_{\text{data}}} [e^{-t\|\hat{f}(\mathbf{u}) - \hat{f}(\mathbf{v})\|^2}], \quad t = 2 \quad (15)$$

More negative values indicate that embeddings are spread more uniformly over the unit hypersphere, which prevents representational collapse.

### 6. Probe Gap [Conneau and Kiela, 2018].

$$\Delta_{\text{probe}} = \text{acc}_{\text{semantic}} - \text{acc}_{\text{token}} \quad (16)$$

The semantic probe trains a linear classifier to predict the downstream task label from the frozen embedding; the token probe predicts the most frequent non-special token in the input sentence. A positive gap indicates that the representation encodes task-relevant semantics more strongly than surface-form lexical identity.